World Academy of Science, Engineering and Technology
International Journal of Aerospace and Mechanical Engineering
Vol:12, No:4, 2018

Implementation of State-Space and Super-Element Techniques for the Modeling and Control of Smart Structures with Damping Characteristics

Nader Ghareeb, Rüdiger Schmidt

***Abstract*—**Minimizing the weight in flexible structures means reducing material and costs as well. However, these structures could become prone to vibrations. Attenuating these vibrations has become a pivotal engineering problem that shifted the focus of many research endeavors. One technique to do that is to design and implement an active control system. This system is mainly composed of a vibrating structure, a sensor to perceive the vibrations, an actuator to counteract the influence of disturbances, and finally a controller to generate the appropriate control signals. In this work, two different techniques are explored to create two different mathematical models of an active control system. The first model is a finite element model with a reduced number of nodes and it is called a super-element. The second model is in the form of state-space representation, i.e. a set of partial differential equations. The damping coefficients are calculated and incorporated into both models. The effectiveness of these models is demonstrated when the system is excited by its first natural frequency and an active control strategy is developed and implemented to attenuate the resulting vibrations. Results from both modeling techniques are presented and compared.

***Keywords*—**Finite element analysis, super-element, state-space model.

I. Introduction

IN modern engineering, weight optimization has always the highest priority during the design of structures. On one hand, it has the advantage of minimizing the amount of raw material used and thus reducing the manufacturing and operational costs. On the other hand, this results in lower stiffness and less internal damping and thus, the structures become more sensitive to vibrations. These vibrations, which are usually introduced by external disturbances, can lead to additional unwanted noise, a decrease in stability, and even to the failure of the structure itself [1]. One of the means to overcome this problem is the implementation of active or smart materials which can be controlled in accordance to the disturbances or oscillations that are sensed by the structure. Structures with these smart elements are then called smart structures. Recent innovations in smart materials coupled with developments in control theory have made it possible to control the dynamics of the concerned structures. This field has experienced a big growth in terms of research and development [2]. The coupled electromechanical properties of the smart materials, used in this work in form of piezoelectric ceramics, make them well suited for use as distributed sensors and actuators for controlling structural response. In the sensor application, mechanically induced deformations can be determined from measurement of the induced electrical potential (direct piezoelectric effect), whereas in actuator applications deformation or strains can be controlled through the introduction of appropriate electric potential (converse piezoelectric effect) [3]. At the beginning, active vibration control has been applied on ships [4]. The first control technique was to reduce the vibrations on a steam ship by synchronizing two engines in opposite phase [5]. Aircraft and spacecraft have had a great impact on investigations in active control of structural vibration as well. The damping of air craft skin or other parts vibration was performed by dampening the critical vibrations with power transmitted by supersonic waves which may be controlled with an electric or a quartz crystal oscillator [6]. The rapid development in this field lead later to the use of point actuators and sensors to control flexible systems based on the knowledge of the elastic mode frequencies and mode shapes at their location [7]. Although the piezoelectric effect was firstly mentioned by Haüy in 1817, demonstrated by Pierre and Jacques Curie in 1880, yet the use of piezoelectric materials as actuators and sensors for noise and vibration control has been demonstrated extensively over the past 30 years [8]. Bailey [9] designed an active vibration damper for a cantilever beam using a distributed parameter actuator which was a piezoelectric polymer. Bailey and Hubbard [10] developed and implemented three different control algorithms to control the cantilevered beam vibration with piezoelectric actuators. On the other hand, Crawley and de Luis [11] and Crawley and Anderson [12] presented a rigorous study on the stress-strain-voltage behavior of piezoelectric elements bonded to beams. Moreover, they observed that the effective moments resulting from piezoelectric actuators can be seen as concentrated on the two ends of the actuator when the bounding layer is assumed to be very thin.

Many other researchers have also performed significant research on the implementation and use of the piezoelectric actuators like [13]-[15]. All these works emphasize the capabilities and applications of piezoelectric elements as distributed vibration actuators and sensors by simultaneously controlling a finite number of modes. It must be mentioned here that most of the investigations done in this field were based either on experimental results from the laboratory, or on using physical laws to derive the structural analytical model of the smart structure. Moreover, the damping coefficients are

N. Ghareeb is with the Mechanical Engineering Department, Australian College of Kuwait, Kuwait (e-mail: n.ghareeb@ack.edu.kw).
R. Schmidt is with the RWTH Aachen University of Technology, Aachen, Germany.

not calculated but rather assumed, which may not reflect the exact performance of the real model.

In the present work, the finite element (FE) method is used. The work comprises the modeling and design of active linear controller to control the vibrations of a smart beam at its tip when its excited with its first natural frequency. Firstly, the piezoelectric actuator is modeled and the relation between voltage and moments at its ends is derived. After that, a modified finite element (FE) model of the smart beam based on the first order shell deformation theory (Mindlin theory) is created. The damping coefficients are then calculated and added to it prior to the reduction to a super element (SE) model with a finite number of degrees of freedom (DOF). Both FE- and SE models are validated by performing a modal analysis and comparing the results with those from the experiments. With the help of a suitable FORTRAN-code, the state-space model is extracted from the SE model. In the last step, a controller based on the Lyapunov stability theory is defined and implemented on both the SE- and the state-space model of the smart beam. Results from both models are shown and then compared. The FE-Program SAMCEF® is used for the creation of the FE and SE models, and MATLAB-SIMULINK® is used for the implementation of the controllers in the state-space model.

II. Modeling

The corresponding analytical model of any structure can be derived either from physical laws (i.e. Newton's motion laws, Lagrange equations of motion, etc.), or from test data using system identification methods (stochastic subspace identification, prediction error method, etc.), or by using the FE modeling [16]. In this work, the FE modeling is used. The smart beam which will be investigated consists of a steel beam, a bonding layer and an actuator (Fig. 1).

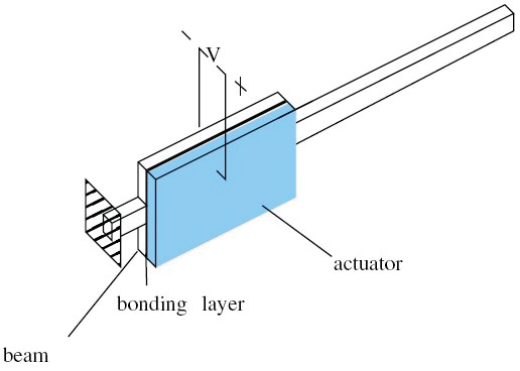

Fig. 1 The smart beam

A. Actuator Modeling

The application of an actuator means the implementation of an appropriate electric potential to control the vibrations or strains in smart structures (converse piezoelectric effect). Commercial FE programs do not give the possibility to create finite elements with electrical DOF. However, the voltage which is applied by the actuator can be replaced by two

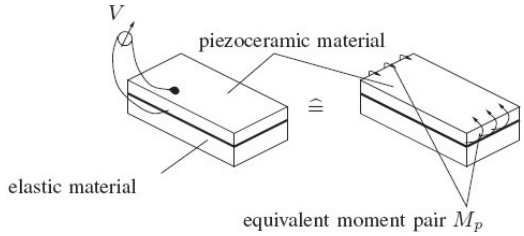

Fig. 2 The induced stresses from a piezo-ceramic actuator lead to the same effect as a moment pair

equal moments concentrated at its end [13]. The piezoelectric material used is assumed linear throughout this work. The relation between actuator moments and voltage will be derived and the moments will then act as the controlling forces on the smart structure (Fig. 2).

Taking the schematic layout of the middle part of the smart beam (Fig. 3) and considering a one dimensional deformation, if a voltage V is applied across the piezoelectric actuator which is composed of a piezo-ceramic material, a piezoelectric strain ϵ_p will be introduced in the piezo as:

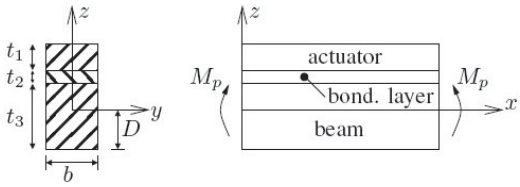

Fig. 3 A schematic layout of the composite beam

$$\epsilon_p = \frac{d_{31}}{t_1} \cdot V \tag{1}$$

V is the voltage of the piezoelectric actuator, d_{31} is the electric charge constant and t_1 is the thickness of the piezoelectric layer.

The longitudinal stress is expressed with Hooke's law as:

$$\sigma_p = E_1 \cdot \epsilon_p \tag{2}$$

where E_1 is the Young's modulus of elasticity of the piezo.

This stress generates a bending moment M_p around the neutral axis of the composite beam given by:

$$M_p = \int_{(t_2+t_3-D)}^{(t_1+t_2+t_3-D)} \sigma_p \cdot b \cdot z \, \mathrm{d}z \tag{3}$$

where t_2 is the thickness of adhesive layer, t_3 is the thickness of beam, b is the width of the composite layer at the beam middle, and D is the distance between the beam bottom and the neutral axis.

Considering moment equilibrium about the neutral axis:

$$\int_{beam} \sigma_{beam} \, \mathrm{d}A + \int_{adh.} \sigma_{adh.} \, \mathrm{d}A + \int_{piezo} \sigma_{piezo} \, \mathrm{d}A = 0 \tag{4}$$

this means:

$$E_3 b \int_{(-D)}^{(t_3-D)} z \, \mathrm{d}z + E_2 b \int_{(t_3-D)}^{(t_2+t_3-D)} z \, \mathrm{d}z +$$

TABLE I
PARAMETERS OF THE COMPONENTS OF SMART BEAM

	Beam	Bonding Layer	Actuator
Material	steel	epoxy resin	PIC 151
Thickness $[mm]$	0.5	0.036	0.25
Density $[kg/m^3]$	7900	1180	7800
Young's mod. $[MPa]$	210000	3546	66667

TABLE II
VALIDATION OF ELEMENT-TYPE BASED ON THE MODAL ANALYSIS

	FE model	Experiment
1^{st}eigenfrequency [Hz]	13.81	13.26
2^{nd}eigenfrequency [Hz]	42.67	41.14

$$E_1 b \int_{(t_2+t_3-D)}^{(t_1+t_2+t_3-D)} z \, \mathrm{d}z \;=\; 0 \tag{5}$$

hence, t_1 is the thickness of the beam, E_2 and E_3 are the Young's modulus of the adhesive and the beam.

After integrating (5), the position of the neutral axis D is found:

$$D = \frac{E_1 t_1^2 + 2E_1 t_1 t_2 + 2E_1 t_1 t_3 + E_2 t_2^2 + 2E_2 t_2 t_3 + E_3 t_3^2}{2E_1 t_1 + 2E_2 t_2 + 2E_3 t_3} \tag{6}$$

now, combining (1)-(3) and (6) together will determine the bending moment generated by the piezo M_p as a function of the voltage V:

$$M_p = \frac{E_1 E_2 (t_1 t_2 + t_2^2) + E_1 E_3 (t_3^2 + t_1 t_3 + 2t_2 t_3)}{E_1 t_1 + E_2 t_2 + E_3 t_3} \cdot \frac{d \cdot b}{2} \cdot V \tag{7}$$

since the relation between M_p and V is known now, the actuator moment can be taken instead as input to the controller designed and implemented in the last section of this work.

B. FE Modeling of the Smart Beam

Many applications in structural dynamics can be successful only if they are represented by an accurate mathematical model. One of the methods used to derive such a model is the finite element modeling. The resultant FE model, which is in the form of mass and stiffness matrices, must be faithfully representative so that it can be used for further applications like control analysis or prediction due to proposed structural changes [17]. In order to find the best FE model representing the smart beam, the optimal element type and element size of the FE must be selected. Consequently, a modal analysis of the real beam will be experimentally performed and then the results will be compared to those from the FE with different element types. A detailed geometry of the smart beam is shown (Fig. 4) and the material properties and thickness of each part are represented in (Table I). As already mentioned before, the commercial software package SAMCEF is used for the creation of the FE model [18].

1) FE- Type and Size: Although the smart beam is created as a single part, but it is modeled as a composite shell with three layers. This means, all the three components of the model, i.e. the beam, the bonding layer and the actuator, are all bonded together without any relative slip among the contact surfaces. Consequently, each layer has its own mechanical properties. To validate the choice of the element type, a modal analysis is done and the first two natural frequencies are extracted and compared to those from the experiment as seen in (TABLE II). As a boundary condition, the left edge of the smart beam is clamped. A 8-node thick shell based on the first order shell deformation theory (FOSD) is used in the descritization for the FE model. More information about the FOSD is found in [19], [21]. Concerning the optimal element size to be used, its well known that reducing the element size will improve the solution accuracy. However, especially in the case of large complex structures, the use of excessively fine elements in the FE models may result in unmanageable computations that exceed the memory capabilities of existing computers [22]. From (Table III), it is seen that using an element size less than $1\ mm$ does not make any significant change on the values of the 1^{st} and 2^{nd} natural frequencies of the smart beam. This means, an element size of $1\ mm$ will be the best choice in the FE modeling.

2) Damping Characteristics: While the dynamic behavior of many engineering structures can be predicted by using the FE technique for example, nevertheless, there remains the need to find out their damping behavior. Unfortunately, damping parameters, which are of significant importance in determining the dynamic response of structures, can't be deduced deterministically from other structural properties. For this reason, recurs must be made to data from experiments conducted on completed structures of similar characteristics. Although such data is scarce in general, but its very valuable for studying the phenomenon and modeling of damping [23]. In fact, there are many non-linear damping models available [24]. In this work, the damping is assumed to be viscous and frequency dependent for the sake of convenience and simplicity [25]. A special case of viscous damping is known as the proportional or Rayleigh damping. This model expresses the damping matrix as a linear combination of the mass and stiffness matrices of the undamped model [26]:

$$C \;=\; \alpha M \;+\; \beta K \tag{8}$$

where α and β are real scalars that need to be determined. In fact, there are more than one method to determine them [27], [28]. Yet, a modified form of the method developed by Chowdhury and Shambhu [29] and validated by Giosan [30] will be used in this work.

Writing (8) in the modal form will give:

$$\phi^T C \phi \;=\; \alpha \phi^T M \phi \;+\; \beta \phi^T K \phi \tag{9}$$

hence, ϕ represents the mode shapes and ϕ^T shows their transpose.

Since the mode shapes corresponding to distinct natural frequencies are orthogonal w.r.t. the mass and stiffness matrices, it follows that [14]:

$$\phi_i^T M \phi_j \;=\; \mu_i \delta_{ij} \tag{10}$$

$$\phi_i^T K \phi_j \;=\; \mu_i \omega_i^2 \delta_{ij} \tag{11}$$

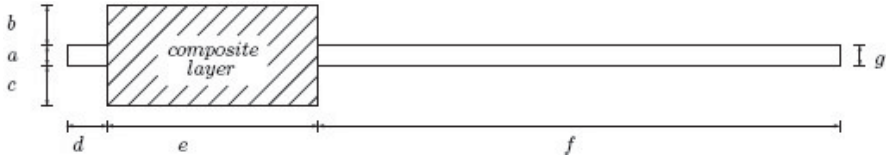

Fig. 4 A detailed geometry of the smart beam [dimensions in mm]

TABLE III
EFFECT OF ELEMENT SIZE ON THE NATURAL FREQUENCY

Element size $[mm]$	1^{st}natural frequency [Hz]	2^{nd}natural frequency [Hz]
0.25	13.80	42.66
0.5	13.81	42.66
1.0	13.81	42.67
2.5	13.83	42.71
5	13.89	42.81
10	14.09	43.21

with μ_i = modal mass of mode i
ω_i = natural frequency of mode i
δ_{ij} = Kronecker-Delta,

$$\delta_{ij} = \begin{cases} 1, & \text{if } i = j \\ 0, & \text{otherwise.} \end{cases}$$

$i =$ no. of modes which is equal to the no. of DOF n.

Since modal shapes are scaled arbitrarily, it is used to normalize them in a way that:

$\mu_i = 1$, with $\phi = (\phi_1, \phi_2, ...\phi_n)$ is the matrix of mode shapes.

The new form of (10) and (11) will be:

$$\phi^T M \phi = diag(\mu_i) = I \tag{12}$$

$$\phi^T K \phi = diag(\mu_i \omega_i^2) = \omega_i^2 \tag{13}$$

Substituting (12) and (13) in (9):

$$\Rightarrow \phi^T C \phi = \bar{C} = \alpha I + \beta \Lambda \tag{14}$$

where, $I = \begin{Bmatrix} 1 & \dots & 0 \\ \vdots & \ddots & \vdots \\ 0 & \dots & 1 \end{Bmatrix}$ and $\Lambda = \begin{Bmatrix} \omega_1^2 & & \\ & \ddots & \\ & & \omega_n^2 \end{Bmatrix}$

Thus, $\bar{C} = \phi^T C \phi$ will become a diagonal matrix, and this is mainly the advantage of this representation.

From (14):

$$\bar{C} = \alpha + \beta \omega_i^2 \tag{15}$$

critical damping $C_c = 2\sqrt{KM} = 2\omega_i M$

modal critical damping $\bar{C}_c = \phi^T C \phi = 2\omega_i \phi^T M \phi = 2\omega_i$

the modal damping ratio is defined as $\xi_i = \dfrac{\bar{C}}{\bar{C}_c}$

this results in:

$$\xi_i = \frac{1}{2}\left(\frac{\alpha}{\omega_i} + \beta \omega_i\right) \tag{16}$$

the objective now is to compute the Rayleigh damping coefficients α and β , and then to substitute them in (8) in order to calculate C.

To solve (16) for α and β , atleast two values for ξ_i with the corresponding values for ω_i are needed. Here, the first mode will be considered, i.e. ξ_1 and ω_1, as well as the mode by which almost 95% of the mass has participated. The damping ratio and the frequency at this mode are called ξ_m and ω_m. The data file of any FE software shows the mass participation of each mode. Thus, ω_1 and ω_m can be read, as well as the mode number m.

A typical plot of (16) is shown in Fig. 5 [20].

The first portion of the curve in this figure shows non-linearity (frequency range: $0.1 - 5$ Hz), and in this case the damping is called "mass proportional damping" where α is much greater than β. Beyond this portion, the curve is linear (frequency range: > 5 Hz). The damping is then called "stiffness proportional damping" and β has a big value. The methodology to calculate α and β can be summarized as follows:

1) After m is found, a modal frequency analysis of the FE model is performed and results are tabulated up to the $2.5 \times m^{th}$ mode.
2) Using results of the experimental modal analysis, ξ_1 can be calculated from the step response FFT of the real model. To do this, it can be referred to [31] for example.
3) At the m^{th} mode, the value of ξ_m can be assumed to be between 2% and 10%, depending on the structure's type and application (mechanical, civil, etc.) [29].
4) With values of (ξ_1, ω_1) and (ξ_m, ω_m), all values of ξ_i can be calculated and then plot based on linear interpolation of the expression:

$$\xi_i = \frac{\xi_m - \xi_1}{\omega_m - \omega_1}(\omega_i - \omega_1) + \xi_1 \tag{17}$$

5) Using the data of (ξ_1, ω_1) and (ξ_m, ω_m), and based on the equation:

$$\beta = \frac{2\xi_1\omega_1 - 2\xi_m\omega_m}{\omega_1^2 - \omega_m^2} \tag{18}$$

back-substituting β in (16) gives α.
6) Next, a second set of data is selected. Its based on: (ξ_1, ω_1) and ($\xi_{2.5m}$, $\omega_{2.5m}$) .
7) β and then α are recalculated as done in steps 5 & 6

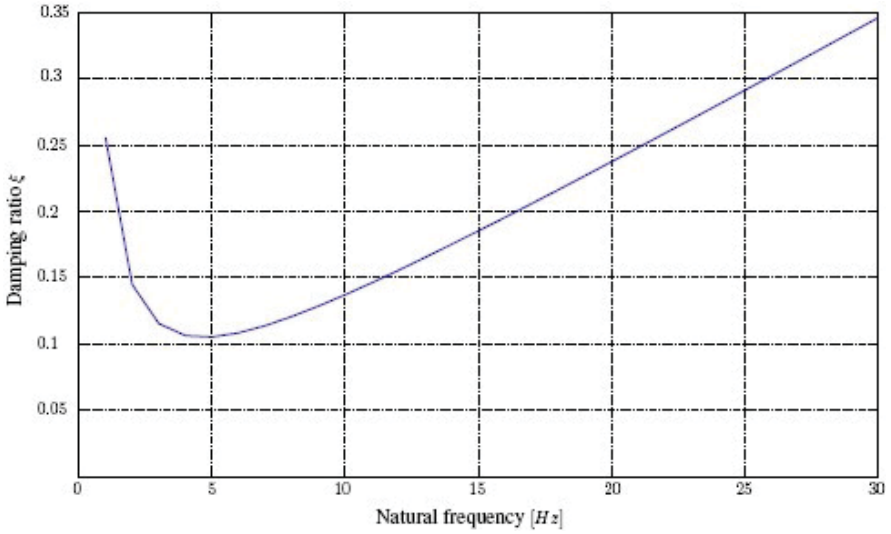

Fig. 5 Variation of the damping ratio with natural frequency of a system

8) A fourth set of data based on the average values of α and β from steps 5 & 7 is obtained.
9) The last three sets of data based on (16) are plotted.
10) Data which fits best with the linear interpolation curve for the first m significant modes is checked.
11) Based on the previous step, the desired values of α and β which give the incremental damping ratio based on Rayleigh damping are selected.

Concerning the smart beam considered in this work, it was found that the first set of data i.e. ($\xi_1,\ \omega_1$) and ($\xi_m,\ \omega_m$) complies with the linear interpolation curve better than the other data. Thus:

$$\alpha\ =\ 0.02577, \text{ and } \beta\ =\ 9.918e^{-6}$$

III. The Super Element Technique

The main objective of the SE technique (also called substructure technique) is the ability to perform the analysis of a complete structure by using results of prior analysis of different regions comprising the whole structure. When a preliminary analysis of the different parts is performed, the computation time and the size of the whole system will be drastically reduced. Moreover, all DOF considered useless for the final solution will be condensed and the rest will be retained. This means, the DOF of the whole system will correspond to the retained nodes plus a number of internal deformation modes (dynamic analysis problems).

The SE techniques has also its drawbacks. The stiffness matrix of the substructures will be saved externally and it can't be changed during the analysis of the whole structure. The stiffness and mass matrices will be saved in a database file, which will need much space of the hard disk once the number of substructures will increase. In addition, no much information is available about the connection between SEs created to form the main structure. More about this topic is available in the SAMCEF tutorials [21]. To construct a SE or, in other words, to remove the unwanted nodes and DOF from the substructure, more than one method can be used. An example of these methods are the "Guyan reduction technique" [32], and the "Component-mode method" which is used in this work.

A. The Component-Mode Method

This method, also called Craig-Bampton method, was initially developed by R. Craig and M. Bampton [33]. The basic idea of it is to split the basic substructure into a certain number of substructures. The DOF of each substructure are then classified into boundary DOF and internal DOF. The boundary DOF are shared by several substructures, while the internal DOF belong only to the considered substructure.

The behavior of each substructure is described by the combination of two types of component modes, the constrained modes and the normal vibration modes. The former are determined by assigning a unit displacement to each boundary DOF while all other boundaries DOF are being fixed. The latter correspond to the vibration modes obtained by clamping the structure at its boundary.

It is thus assumed that the behavior of the substructure in the global system can be represented by superimposing the constrained modes and a small number of normal modes. Hence, by retaining only the low-frequency vibration modes, the substructure's dynamic deformed shape is represented with sufficient accuracy. This method is discussed in details in [34].

B. SE Modeling

Before the SE is created, the retained nodes and the condensed nodes must be designated, and the number of internal modes to be used must be specified. Once again, the number of modes must correspond to at least 95% participation of the mass. The retained nodes are usually those where boundary conditions are added, or where stresses, displacements,...etc. are imposed or measured. In the current work, ten internal modes are used and the retained nodes are those where the clamp is added and the actuators and sensors are placed. All other nodes will be condensed. Concerning

TABLE IV
COMPARISON BETWEEN FE AND SE MODEL

	FE model	SE model
Number of nodes	8206	5
Number of elements	2575	1
DOF	49236	34

the smart beam used in this work, there are five retained nodes in the SE model (Fig. 6), and they comprise:

- a clamp constraint on node 1
- the actuator moments, i.e. the control forces, on nodes 2 and 3
- an additional sensor to measure the vibrations on node 4 (it will be used in future works)
- a sensor to measure the vibrations on node 5

Fig. 6 The retained nodes of the super element

C. Comparison between FE and SE Model

The number of nodes, elements and DOF of SE and FE models are listed in (Table IV). It is clear that the number of elements, nodes, and DOF was reduced. This lead also to a smaller structure and less computation time.

D. Validation of the SE Model

In order to validate the SE model, modal analysis is performed and results are compared to those from the FE model (Table V). It is clear that the results of modal analysis on both models did not show a big difference on the first four natural frequencies. Since the controller will be designed to control the vibrations after exciting the model with its first natural frequency only, further readings are not necessary.

IV. THE STATE SPACE MODEL

The fundamental equation describing the dynamic behavior of a damped structure discretized by the FE method is written in the form:

$$M\ddot{q}(t) \; + \; C\dot{q}(t) \; + \; Kq(t) \; = \; f(t) \qquad (19)$$

where $q(t)$ is the state vector which collects the displacements of the structure by DOF, and $f(t)$ is a vector expressing the applied loads. If the total number of DOF of the FE model is n, then the dimension of the state vector $q(t)$ will be also equal to n, and that of the mass, stiffness and damping matrices will be $n * n$. In this work, n will be 49236 if the full FE model will be used. However, since a SE was constructed, and the desired results concern specific locations of the structures only, n was reduced to s, where $s \; = \; r \; + \; m \; - \; 6$.

r is the number of retained nodes, m is the number of internal modes chosen, and the number 6 corresponds to the rigid body modes that will be automatically eliminated. The new form of the mass, stiffness and damping matrices will have the size $s \times s$, which is 34 in case of the smart beam. The state-space model is written according to (19) with dimensions of the SE model. The general form is:

$$\dot{x} \; = \; Ax \; + \; Bu, \text{ and } y \; = \; Cx \; + \; Du$$

the state vector x, the input vector u and the output vector y are defined as:

$$x \; = \; \begin{Bmatrix} q \\ \dot{q} \end{Bmatrix} \qquad u \; = \; \{F\}, \qquad y \; = \; \begin{Bmatrix} q_{out} \\ \dot{q}_{out} \\ \ddot{q}_{out} \\ F_{out} \end{Bmatrix}$$

and A, B, C and D are called the system state-space representation and F is the external load applied. So that:

$$A = \begin{bmatrix} 0 & I \\ -M^{-1}K & -M^{-1}B \end{bmatrix}, \; B = \begin{bmatrix} 0 \\ -M^{-1} \end{bmatrix}$$

$$C = \begin{bmatrix} I & 0 \\ 0 & I \\ -M^{-1}K & -M^{-1}B \\ 0 & 0 \end{bmatrix}, \; D = \begin{bmatrix} 0 \\ 0 \\ M^{-1} \\ I \end{bmatrix}$$

$\text{size}\,(A) = \; 2s \times 2s, \quad \text{size}\,(B) = \; 2s \times in$
$\text{size}\,(C) = \; out \times 2s, \quad \text{size}\,(D) = \; out \times in$

where out is the no. of outputs from the system, and in is the no. of inputs to the system.
By using a FORTRAN code, and upon specifying the types and positions of inputs and outputs, the state-space model was extracted.

V. CONTROLLER DESIGN

The performance of smart structures for active vibration control depends strongly on the control algorithm accompanied by it. As outlined previously, one of the objectives of this work is to design a controller which is able to damp the first vibrational mode of the smart beam. The beam is excited with its first natural frequency and then it is left to vibrate freely. At the moment when free vibration begins, the controller is activated. Concerning the control algorithm, the Lyapunov stability theorem is used. It is assumed here that damping the first natural frequency will not affect other natural frequencies which are not investigated in this work.

A. Lyapunov Stability Theorem

Although there is no general procedure for constructing a Lyapunov function, yet any function can be considered as a candidate function if it meets some requirements, i.e. if its positive definite, equal to zero at the equilibrium state and if its derivative is less or equal to zero [35].
In this work, the energy equation of a thin Bernoulli-Euler beam (20), which is modeled as one FE in a one-dimensional system with length h and left point coordinate x_i, will be considered as the Lyapunov function candidate.

$$U \; = \; \frac{1}{2} \int_{x_i}^{x_{i+h}} \left[\rho \Big(\frac{\partial y}{\partial t} \Big)^2 \; + \; EI \Big(\frac{\partial^2 y}{\partial x^2} \Big)^2 \right] \mathrm{d}x \qquad (20)$$

TABLE V
COMPARISON BETWEEN THE FIRST FOUR NATURAL FREQUENCIES

No. of natural frequency	FE model (Hz)	SE model (Hz)	% Error
1	13.811	14.249	3.07
2	42.673	43.414	1.71
3	145.49	152.54	4.62
4	150.16	154.38	2.73

This function is locally positive definite, it is continuously differentiable and equal to zero at the equilibrium state. Yet, according to the last requirement for Lyapunov functions, the derivative of this function (21) must be smaller or less than zero too.

$$\dot{U} = \int_{x_i}^{x_{i+h}} \left[\rho \dot{y} \ddot{y} + EI \frac{\partial^2 y}{\partial x^2} \frac{\partial}{\partial t} \left(\frac{\partial^2 y}{\partial x^2} \right) \right] \mathrm{d}x \qquad (21)$$

Substituting the derived equations for the bending moment M, shear force V, and after assuming no shear [32], the first derivative will become:

$$\dot{U} = M \left(\dot{y}\prime_{x_i+h} - \dot{y}\prime_{x_i} \right) \qquad (22)$$

to ensure that (22) is always smaller or equal to zero, the actuator moment M can have the value:

$$M = -k \left(\dot{y}\prime_{x_i+h} - \dot{y}\prime_{x_i} \right) \qquad (23)$$

where k is a positive constant. Subst. (23) in (22) yields:

$$\dot{U} = -k \left(\dot{y}\prime_{x_i+h} - \dot{y}\prime_{x_i} \right)^2 \leq 0 \qquad (24)$$

in this case, (23) can be used as the controller for the smart beam. The intention of the current work is to design a functional controller and not an optimal one, thus $k = 30$ is used and the controller is implemented in the SE and the state-space models.

1) SE Model with Controller: There are many ways to add a controller to a SE model in SAMCEF. In this work, the nonlinear forces element (FNLI) is used [21]. This element enables the insertion of a list of n general linear or nonlinear internal forces as a function of a list of n DOF and their derivatives. Concerning the smart beam used in this work, two equal moments at nodes 2 and 3 (but with opposite directions) were added, where each one of them is a function of the velocities at both nodes according to (23).

The beam was excited with its 1^{st} natural frequency, and then it was left to vibrate freely (Fig. 7). At the moment when free vibrations started ($t = 20\ s$), the controller was activated. Three different values for the constant k were used for the controller design, and results are shown in (Fig. 8). The implementation of the controller changed the natural frequency of the system as well. In the FFT spectrum diagram (Fig. 9), the effect on the natural frequency of the smart beam and its magnitude is illustrated.

2) State-Space Model with Controller: In the state-space representation of the smart beam, MATLAB/SIMULINK is used to design and implement the controller. However, two steps must be done. In step one, the only input is the forced excitation with the first natural frequency, and the output contains the state vectors which will be fed as initial conditions in the second step. In the second step, the input consists of the two actuator moments, and the output comprises the tip displacement at the fifth node and the velocities at the second and third nodes (Fig. 10). Based on the Lyapunov stability theorem, the last two outputs, multiplied by a constant k are fed back as actuator moments in different directions. The results are depicted in (Fig. 11).

3) Comparison of Results from SE Model and State-Space Model: The controller has been implemented on both models and the results were almost the same. This can be seen in the case when the constant $k = 5$ for example. Yet, if the curves are slightly zoomed, a very small difference appears (Fig. 12). This is because the time steps used in both models were different. It was not possible to use a fixed time step in the state-space model. Using a SE model decreased the simulation time, although more results (like stresses, energy curves, etc) could be gleaned out from it. However, the controller could be easier designed and implemented in the state-space model.

VI. CONCLUSIONS AND FUTURE WORKS

In this work, the basic procedures for modeling and simulation of a smart beam were presented. At the beginning, the relation between actuator velocity and actuator moments was derived. A FE model was created and the damping coefficients were calculated using data from experimental results. A SE model was then deduced from the FE model and then the state-space model was derived. A controller based on the Lyapunov stability theory was designed and implemented to control the free body vibrations of the smart beam once excited by its first natural frequencies. Results from both models were shown and compared.

In the future, other types of controllers will be used. Nevertheless, more natural frequencies will be controlled and the possibility to implement the controllers experimentally will be investigated.

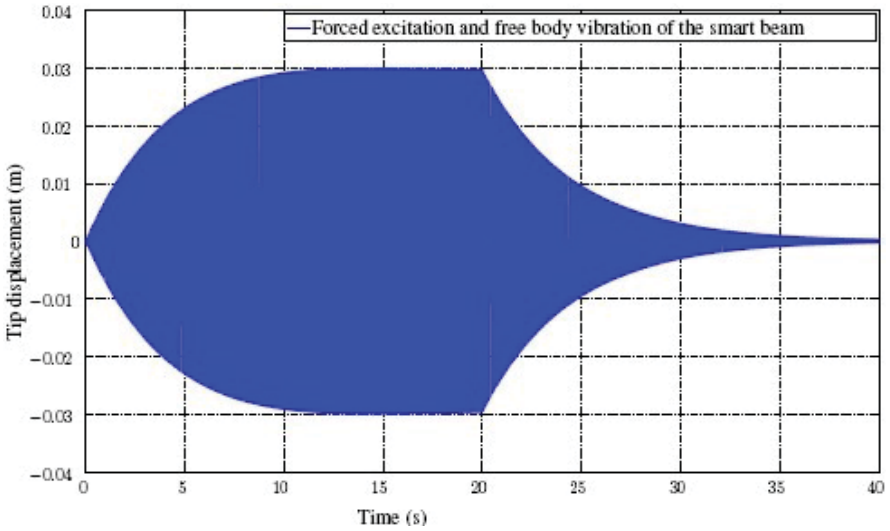

Fig. 7 Forced excitation (till t=20s) and free body vibration of the smart beam

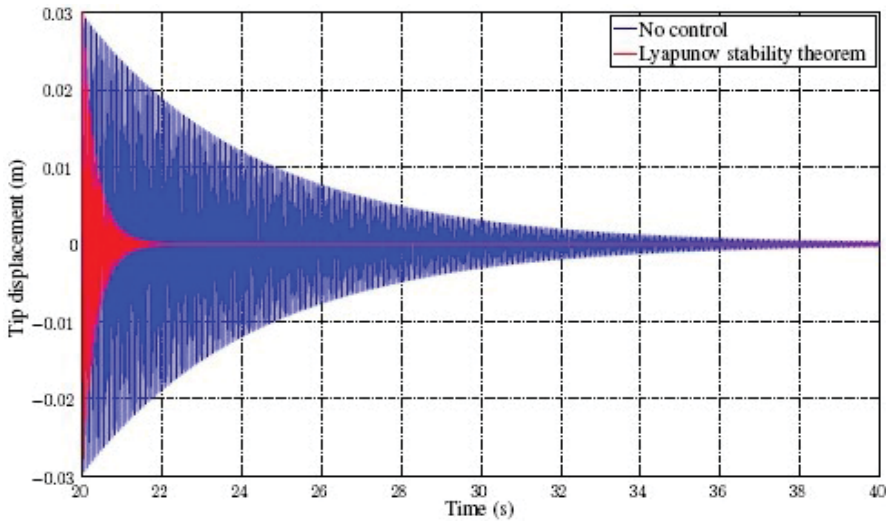

Fig. 8 Tip displacement vs. time with and without controller during the free vibration (SE model is used)

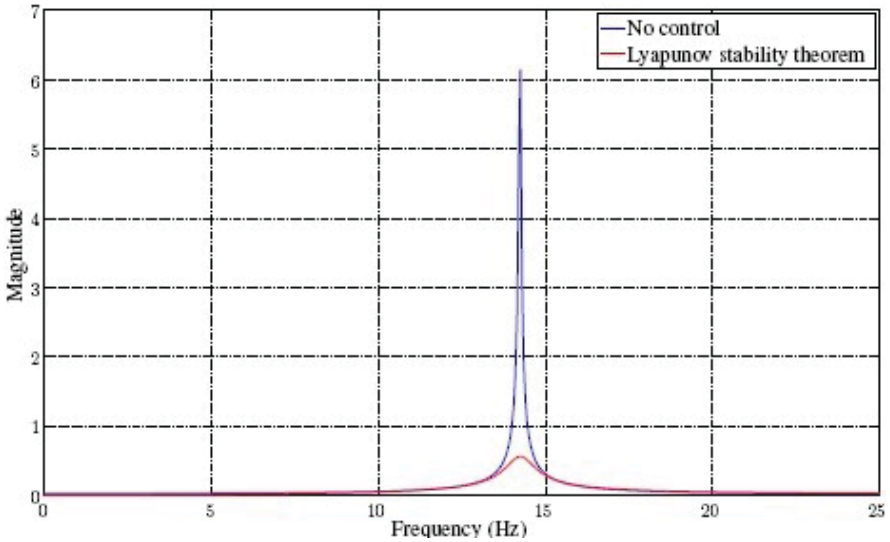

Fig. 9 The FFT spectrum of the smart beam

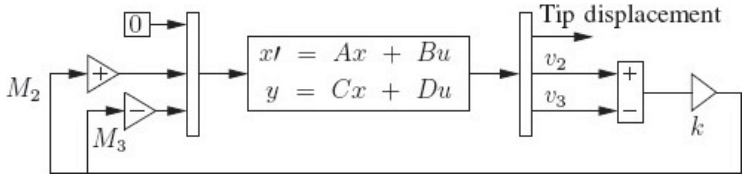

Fig. 10 The state-space model of the smart beam with controller

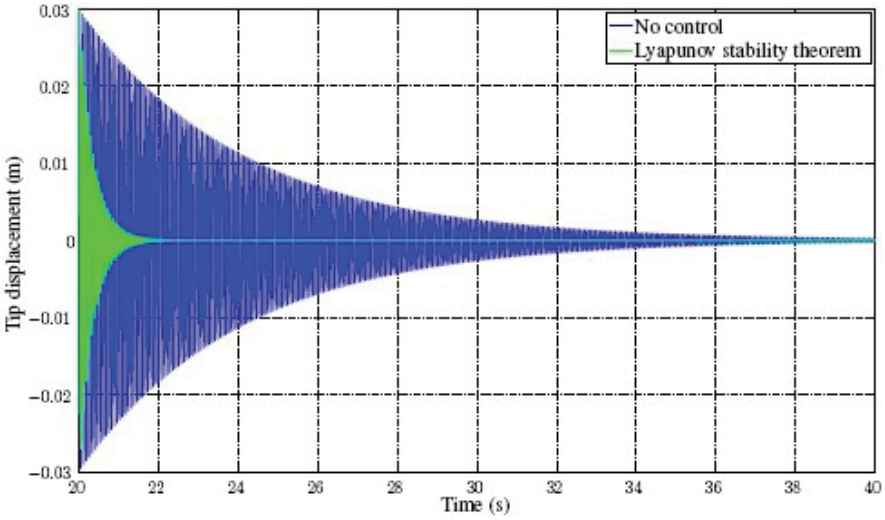

Fig. 11 Tip displacement vs. time with and without controller during the free vibration (state-space model is used)

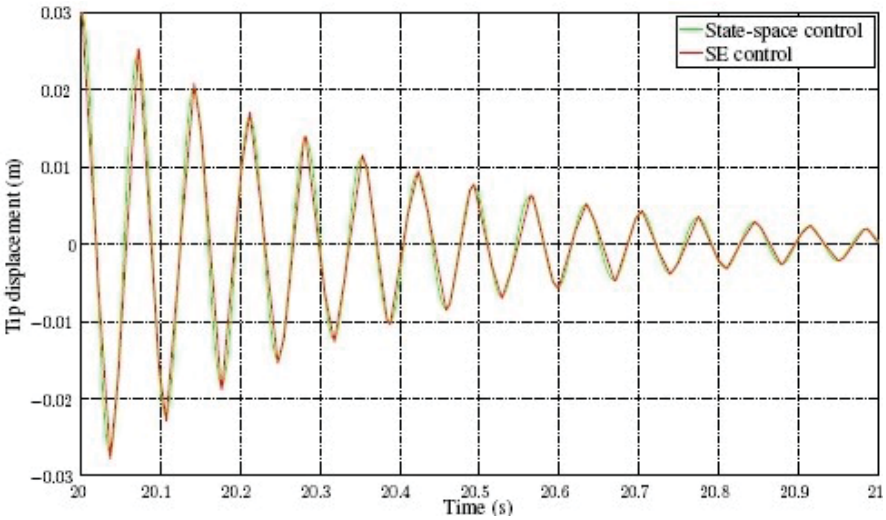

Fig. 12 Tip displacement vs. time using the SE and the state-space models

REFERENCES

[1] N. Ghareeb and Y. Radovcic, "Fatigue Analysis of a Wind Turbine Power Train", *DEWI magazin*, Germany, August 2009, pp 12-16.

[2] R. Vepa, "Dynamics of Smart Structures", *John Wiley & Sons*, 2010.

[3] S. Narayanan and V. Balamurugan, " Finite Element Modeling of Piezolaminated Smart Structures for Active Vibration Control with Distributed Sensors and Actuators", *Journal of Sound and Vibration*, 2003, vol. 262, pp 529-562.

[4] A. Mallock, "A Method of Preventing Vibration in Certain Classes of Steamships", *Trans. Inst. Naval Architects*, 1905, 47, pp 227-230.

[5] H. Hort, "Beschreibung und Versuchsergebnisse ausgeführter Schiffsstabilisierungsanlagen", *Jahrb. Schiffbautechnik Ges.*, 1934, 35, pp 292-312.

[6] A. Vang, "Vibration Dampening", *U.S. Patent US 2,361,071*, Oct. 24, 1944.

[7] M. Balas, "Active Control of Flexible Systems", *Journal of Optimization theory and Applications*, 1978, vol. 25, no. 3, pp 415-436.

[8] V. Piefort, "Finite Element Modelling of Piezoelectric Active Structures", *Universit Libre de Bruxelles, PhD Thesis*, Belgium, 2001.

[9] T. Bailey, "Distributed-Parameter Vibration Control of a Cantilever Beam Using a Distributed-Parameter Actuator", *Massachusetts Institute of Technology, Msc. Thesis*, 1984.

[10] T. Bailey and J. Hubbard Jr., "Distributed Piezoelectric-Polymer Active Vibration Control of a Cantilever Beam", *AIAA Journal of Guidance and Control*, 1985, vol. 6, no. 5, pp. 605-611.

[11] E. F. Crawley and J. de Luis, "Use of Piezoelectric Actuators as Elements of Intelligent Structures",*AIAA Journal*, 1987, vol. 25, no. 10,

pp 1373-1385.
[12] E. Crawley and E. Anderson, "Detailed Models of Piezoceramic Actuation of Beams", *Journal of Intelligent Material Systems and Structures*, 1990, vol. 1, no. 1, pp. 4-24.
[13] J. Fanson and J. Chen, "Structural Control by the Use of Piezoelectric Active Members", *Proceedings of NASA/DOD Control-Structures Interaction Conference*, 1986, NASA CP-2447, part2, pp. 809-830.
[14] A. Preumont, "Vibration Control of Active Structures, An Introduction", *Kluwer Academic Publishers*, 2002.
[15] S. Moheimani and A. Fleming, "Piezoelectric Transducers for Vibration Control and Damping", *Springer*, 2006.
[16] W. Gawronski, "Advanced Structural Dynamics and Active Control of Structures", *Springer*, 2004.
[17] J. He and Z. Fu, "Modal Analysis", *Butterworth-Heinemann*, 2001.
[18] SAMTECH Products, *www.samtech.com*.
[19] S. Kapuria, G. Dube and P. Dumir, "First-Order Shear Deformation Theory Solution for a Circular Piezoelectric Composite Plate under Axisymmetric Load", *Smart Materials and Structures*, 2003, vol. 12, pp. 417-423.
[20] J. F. Semblat, "Rheological Interpretation of Rayleigh Damping", *Journal of Sound and Vibration*, 1997, vol. 5, pp. 741-744.
[21] I. Kreja and R. Schmidt, "Large Rotations in First-Order Shear Deformation FE analysis of Laminated Shells", *International Journal of Non-Linear Mechanics*, 2006, vol. 41, pp. 101-123.
[22] W. Ko and T. Olona, "Effect of Element Size on the Solution Accuracies of Finite-Element Heat Transfer and Thermal Stress Analysis of Space Shuttle Orbiter", *NASA Technical Memorandum 88292*, 1987.
[23] J. Butterworth, J. Lee and B. Davidson, "Experimental Determination of Modal Damping From Full Scale Testing", 13^{th} *World Conference on Earthquake Engineering*, Vancouver, Canada, August 1-6, 2004, Paper no. 310.
[24] A. Puthanpurayil, R. Dhakal and A. Carr, "Modelling of In-Structure Damping: A review of the State-of-the-art", *Proceedings of the Ninth Pacific Conference on Earthquake Engineering*, Auckland, New Zealand, 14-16 April, 2011
[25] A. Alipour and F. Zareian, "Study Rayleigh Damping in Structures; Uncertainties and Treatments", *The* 14^{th} *World Conference on Earthquake Engineering*, Beijing, China, October 12-17, 2008.
[26] L. Rayleigh, "Theory of Sound (two volumes)", *Dover Publications*, New York, 1877.
[27] R. Spears and S. Jensen, "Approach for Selection of Rayleigh Damping Parameters Used for Time History Analysis", *Proceedings of PVP2009, ASME Vessels and Piping Division Conference*, Prague, Czech Republic, July 26-30, 2009.
[28] S. Adhikari, "Damping Models for Structural Vibration", *PhD Thesis*, 2000.
[29] I. Chowdhury and S. Dasgupta, "Computation of Rayleigh Damping Coefficients for Large Systems", *The Electronic Journal of Geotechnical Engineering*, 2003, vol. 8, Bundle 8C.
[30] I. Giosan, "Dynamic Analysis with Damping for Free-Standing Structures Using Mechanical Event Simulation", *Autodesk Report*, 2010.
[31] D. Ewins, "Modal Testing: Theory and Practice", *John Wiley & Sons Inc.*, 1984.
[32] M. Petyt, "Introduction to Finite Element Vibration Analysis", *Cambridge University Press*, 2003.
[33] R. Craig and M. Bampton, "Coupling of Substructures for Dynamic Analyses", *AIAA Journal*, 1968, vol. 6, no. 7, pp 1313-1319
[34] C. Rickelt-Rolf, "Modellreduktion und Substrukturtechnik zur effizienten Simulation dynamischer, teilgeschädigter Systeme", *Technische Universität Carolo-Wilhelmina zu Braunschweig, PhD Thesis*, Germany, 2009.
[35] H. Khalil, "Nonlinear Systems", *Prentice Hall*, Madison, 1996.

Nader Ghareeb received his B.S. Degree in Mechanical Engineering from Beirut Arab University in 2001. After working for one year as HVAC engineer, he joined the RWTH Aachen University in Germany and received the M.Sc. in "Simulation Techniques in Mechanical Engineering" in February 2005. After working for three years in the simulation of wind turbines bed-plates, he returned to the RWTH Aachen University of Technology and received his Ph.D. Degree in Mechanical Engineering in April 2013. In September 2013 he joined the Ausralian College of Kuwait where he currently holds the position of assistant Professor at mechanical engineering department. Dr. Ghareebs research interests are: Active linear control, Smart structures, Multi-body simulation, Finite element analysis, Blast simulation and Wind turbines.

Rüdiger Schmidt is Professor Emeritus at the Faculty of Mechanical Engineering , RWTH Aachen University. Rüdiger does research in Aerospace Engineering, Structural Engineering and Mechanical Engineering. The current project is 'Non-linear analysis of laminated panels.'